Available online at www.sciencedirect.com

ScienceDirect

Procedia CIRP 117 (2023) 299–304

www.elsevier.com/locate/procedia

19th CIRP Conference on Modeling of Machining Operations

Modeling of stresses at the cutting wedge in the interrupted cut for the design of the cutting edge microgeometry

Berend Denkena[a], Benjamin Bergmann[a], Tobias Picker[a], Malte Kraeft[a]*

[a]*Institute of Production Engineering and Machine Tools (IFW), Leibniz Universität Hannover, An der Universität 2, 30823 Garbsen, Germany*

* Corresponding author. Tel.: +49 (0)511 762 12321; fax: +49 (0)511 762 5115. *E-mail address:* kraeft@ifw.uni-hannover.de

Abstract

The wear behaviour of cutting tools can be significantly improved by a load-optimized design of the cutting edge microgeometry. Thereby, the knowledge of local mechanical stresses is necessary. The experimental-based modelling of mechanical stresses in the continuous cut was already investigated in previous work. In this paper, this method is adapted to the interrupted cut by considering contact lengths, process forces and process temperatures during tool entry and exit. The identified mechanical stresses and temperatures are used for a tool material specific cutting edge microgeometry design.

Keywords: turning; cutting tools; cutting edge; mechanical stresses; microgeometry; interrupted cut

1. Introduction

Increasing productivity through cutting edge preparation is state of the art in the manufacture of cutting tools. The microgeometry of the cutting edge has a considerable influence on the tool performance [1]. Denkena et al. [2] developed the form-factor method, which describes not only symmetrical but also asymmetrical cutting edge microgeometries with the parameters S_α, S_γ, Δr, K and φ (Fig. 1). Moreover, the arc lengths l_α and l_γ defined by Bassett can be used to define the cutting edge geometry. These allow a description and comparison of the cutting edge microgeometry under deviating wedge angles [3].

By preparing the cutting edge, a defined microgeometry is established, the mechanical stability is enhanced and the mechanical loads are modified, which leads to lower tool wear [3-6]. Rehe achieved a tool life gain of 98.5% compared to unprepared cutting edges when milling 42CrMo4-QT by a load-optimized design of the cutting edge rounding. [6]

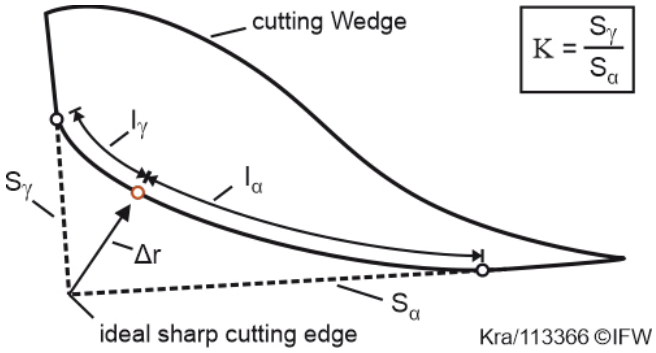

Fig. 1. Cutting edges microgeometry

In order to design the cutting edge microgeometry in a load-optimized way, knowledge of the mechanical and thermal stresses in the tools is required. Known methods to estimate stresses along the cutting wedge are the split tool [7] and tools with restricted contact length [8]. However, with those methods the stresses close to the cutting edge cannot be identified.

10.1016/j.procir.2023.03.051

Furthermore, the stress calculations using the Finite Elemente Method (FEM) [9] strongly depend on the chosen material and friction models.

Bergmann [4] developed a method to calculate the load stresses along the cutting wedge using high speed recordings of contact lengths and process force measurements. In combination with temperature measurements, the results are used for a design method of cutting edge microgeometries.

However, the method was only applied for the continuous cut. Machining with interrupted cutting requires a more stable cutting edge. Currently there is no microgeometry design method for the interrupted cut. To develop such a method, knowledge of the mechanical and thermal stresses in the tool is required. In this paper, a method is presented and applied to transfer the approach of Bergmann to the interrupted cut. For this purpose, load stresses and temperatures are identified for the interrupted cut and used for an application-specific cutting edge design.

2. Experimental setup

The experimental investigations were carried out on a planing test rig with integrated linear direct drive, which enables cutting speeds of up to 500 m/min. The process forces were measured using a Kistler type 9257B multicomponent dynamometer and Kistler type 5015 charge amplifiers.

A high-speed camera Photron Fastcam SA5 was aligned perpendicular to the tool, to analyze the chip formation and tool contact lengths. A sapphire glass was clamped between the camera and the workpiece sample to avoid lateral material flow. To realize an interrupted cut, the specimen geometry shown in Fig. 2 was used with a constant uncut chip thickness h_{konst} = 0.1 mm.

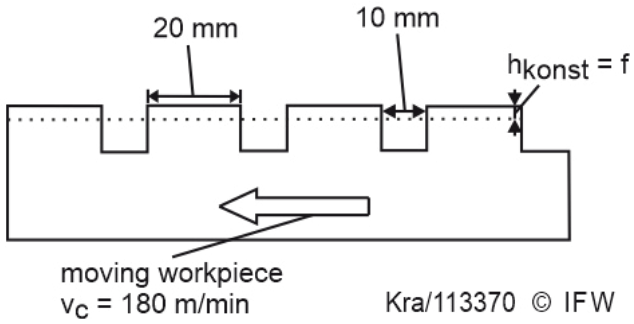

Fig. 2. planing workpiece for interrupted cutting

Along the workpiece length of L = 120 mm, the workpieces had four interruptions. In all investigations, a constant chip width of b = 2 mm and a constant cutting speed of v_c = 180 m/min were maintained. Inserts of the type SNMN 120408 were used. The inserts were clamped in a tool holder with a resulting rake angle γ = -6° and a clearance angle α = 6°. The cutting edge rounding was varied in the range from $\overline{S}$ = 30 µm to $\overline{S}$ = 100. Cemented carbide with a cobalt content of 5% was used as tool material. The tool is coated with a 2 µm thick TiAlN coating. Furthermore, to enhance the recordings of the contact conditions, the specimens were polished and etched on the side facing the camera. To calculate the stresses in the tool, knowledge of the occurring temperatures during machining is necessary. Therefore, the temperature is determined by recording of the thermal radiation (pyrometry). Due to the short process times of the planing process, the temperature measurements were done on Gildemeister CTX520 Linear machine tool. For the temperature measurement, a pyrometer of the type "IGAR12-LO" is used. This pyrometer features a 2-color principle, which allows the temperature to be determined without first determining the emission coefficient of the material. The pyrometer has an acquisition time of 2 ms, which also allows recording of highly dynamic temperature changes. The disadvantage of the measurement method is the required energy of the thermal radiation. Only Temperatures above 350 °C can be recorded. However, it is known from previous investigations [3, 4] that temperatures above 350 °C can be expected in turning of steel, and this measurement method can therefore be used. The experimental setup is shown in Fig. 3.

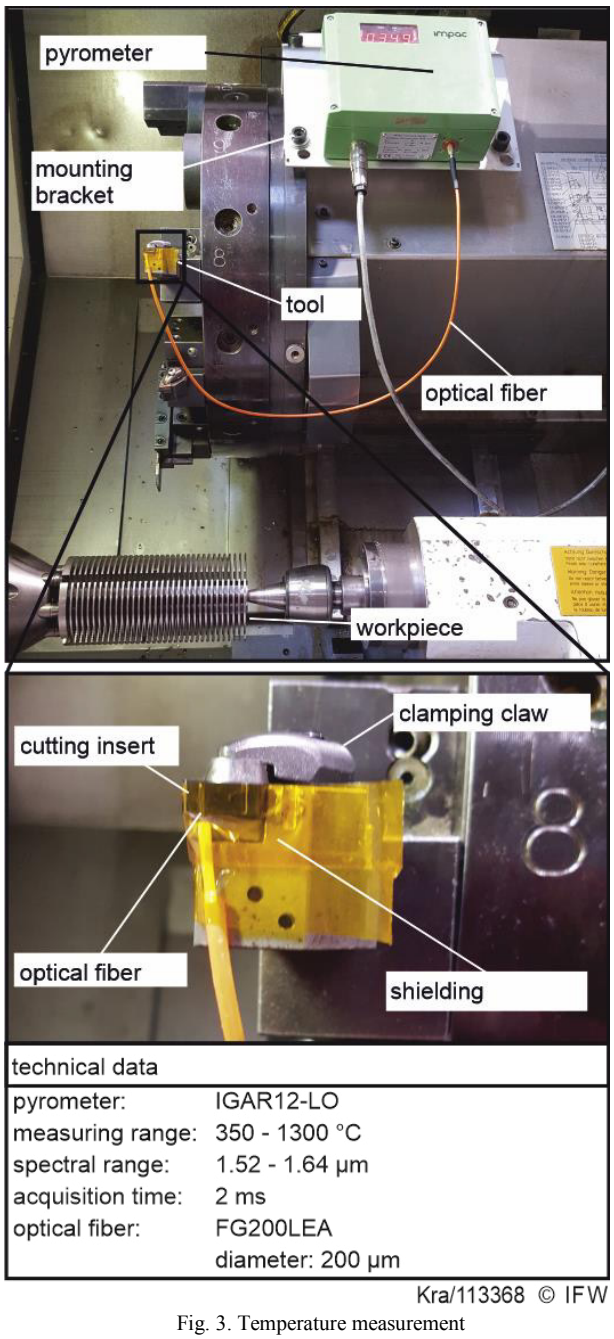

Fig. 3. Temperature measurement

The temperature was measured at nine different positions as shown in Fig. 4. The positioning of the glass fiber was implemented by previously set grooves in the tool. The grooves were created by laser ablation on a Sauer Lasertec 40S. Both, the depth and the distance to the rake face, were varied in order to get a 2-dimensional temperature field. The measuring points were arranged rectangular with an edge length of 0.2 mm. The temperature close to the cutting edge is measured with a distance of 0.2 mm to the flank face and 0.2 mm to the rake face. A quartz fiber FG200LEA from Thorlabs was used to guide the thermal radiation. The fiber has a multilayer cladding that allows it to withstand temperatures and chemicals. Before each measurement, the glass fiber was manually polished and the cladding was removed using a special tool.

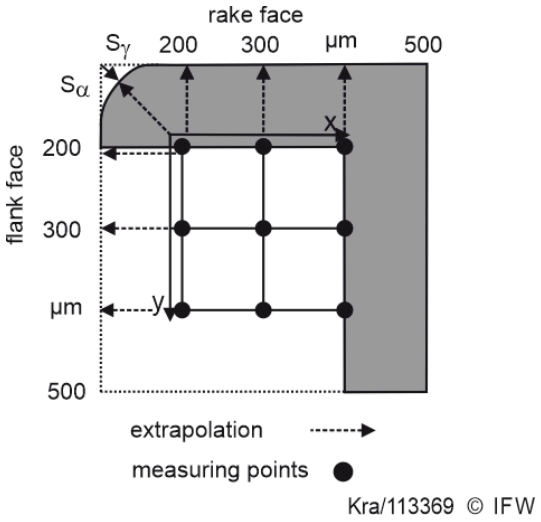

Fig. 4. Temperature measure positions

3. Experimental results

3.1 Contact lengths

Microcinematographic examination of chip formation can be used to determine the contact length at the rake face KL_γ and the minimum chip thickness h_{min}. In continuous chip formation, KL_γ is nearly constant if the chip thickness is constant. In the case of interrupted cutting, the tool entry and exit must also be examined. In Fig. 5, the rake face contact lengths KL_γ and the shear angle are shown in the chip formation images taken during the interrupted cut for tool entry, the continuous state and the tool exit. During the impulsive entry of the tool, the material is strongly plastically deformed until the yield stress of the workpiece is exceeded, and chip formation begins (Fig. 5, top). Due to the geometrical relationship between the set chip thickness h and the rake angle, the initial contact always occurs on the rake face at a distance of 0.11 mm from the flank face. Since no cutting edge rounding is larger than the maximum chip thickness of h = 0.1 mm in the parameter range investigated, the cutting edge rounding is not involved in the first microseconds of entry and accordingly has no effect on the tool-workpiece contact.

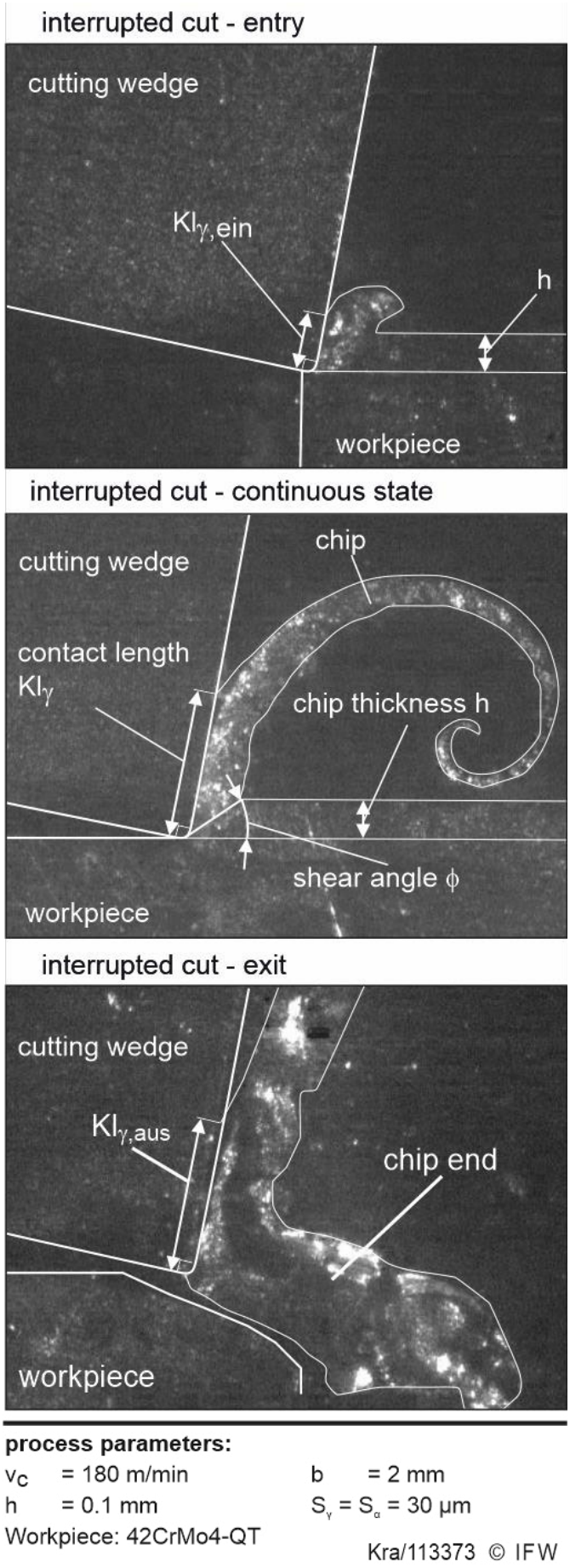

Fig. 5. Chip formation

According to the findings of Klocke, the entry contacts have a great influence on the application behavior during milling or in interrupted cutting [10]. Therefore, different load cases have to be distinguished when evaluating the fracture behavior. If a positive rake angle or an up milling process are considered, the cutting edge or cutting edge rounding hits the workpiece first, and the chip builds up after exceeding the minimum chip thickness. If a negative rake angle or down milling process are considered, the rake face meets the workpiece in an impact-like manner and the flow stress of the material must be exceeded in this area at very high strain rates.

After tool entry, flow chip formation takes place in the continuous as well as in the interrupted cut when machining 42CrMo4-QT. Regardless of the machining process, a shear angle $\phi = 29°$ can be observed. The analysis of the shear angle as a function of the cutting edge rounding shows a deviation of 2°. The change is therefore not significant and the existing mechanisms for chip compression can be applied to flow chip formation according to the findings of Bergmann [4].

Additionally, in the interrupted cut, the chip formation during the tool exit has to be analyzed. According to the findings of Pekelharing and Scherbath, the chip end breaks out at the tool exit. The shape of the chip end depends on the exit angle and the maximum chip thickness. The reason is a crack propagation from the primary shear zone to the end of the workpiece, which leads to a larger segment of the chip to break off during tool exit [11-13]. The chip-end can also be identified in the high speed images of the interrupted machining (Fig. 5, bottom). As the cutting edge microgeometry increases, the chip-end becomes smaller, due to the stronger material deformation in front of the cutting edge and the suppression of crack propagation to the end of the workpiece.

The variation of the cutting edge rounding in the range from $\overline{S} = 30$ µm to $\overline{S} = 100$ µm shows no relevant influence on the contact lengths Kl_γ. With the given process parameters, contact lengths of $Kl_\gamma = 360$ µm were obtained for the continuous cut. For the contact length at the tool exit $Kl_{\gamma,aus} = 420$ µm was determined. The maximum deviation of the measured values is 15 µm. The chip formation as well as the contact lengths are now known with sufficient accuracy.

3.2 Process temperatures

Using the experimental setup for temperature measurements during orthogonal turning, the tool temperature can be recorded during the process. During continuous machining, the temperature rises for the first 1 to 1.5 seconds (heating phase) from the initial temperature $T_0 = 20$ °C to the respective maximum temperature T_{max} of the measuring position. This is then subject to only minor fluctuations and can therefore be assumed to be a stationary temperature.

In case of the interrupted cut there is initially a heating phase and then a stationary temperature as well. This is due to the short times of the cutting interruption of approx. 3 ms in combination with the thermal inertia of the cutting material, which do not lead to any measurable temperature changes between the process conditions with engaged and not engaged tool. Different cutting conditions as well as different cutting edge roundings result in different temperatures T_{max}, but the effects of the cutting conditions and the cutting edge microgeometry on the temperature can still be determined. With the help of the results of these temperature measurements, the temperature fields of different cutting edge microgeometries or process parameters can be determined and compared with each other by varying the measuring points (Fig. 3) and temperature extrapolation according to Bassett [3]. Fig. 6 shows exemplary cutting wedge temperatures with $S_\gamma = S_\alpha = 30$ µm and 60 µm, respectively.

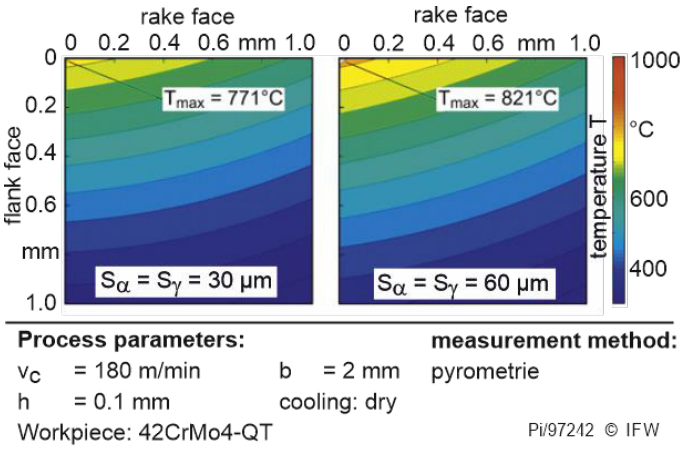

Fig. 6. Temperatures at the cutting wedge

Increasing the cutting edge roundings from 30 to 60 µm increases the maximum tool temperature from 771 °C to 821 °C. The use of larger cutting edge roundings leads to higher maximum temperatures at the cutting wedge. According to the findings of previous works [3, 4], the temperatures at the flank face increase with increasing cutting edge segment S_α or increasing cutting edge arc length l_α, respectively. The higher temperatures are the result of the increase in friction, caused by the greater contact length between the workpiece and tool.

4. Modelling of the mechanical and thermal stresses

During continuous cutting, the stresses can be calculated according to Bergmann [4, 14]. The knowledge of the minimum chip thickness, the elastic chip thickness springback as well as the contact length at the chip surface in combination with the existing process forces allow the calculation of the normal and tangential stresses along the cutting wedge (Fig. 7). From the investigations on interrupted machining, it is clear that the stresses during tool entry and exit must be calculated in addition to the stress distribution during the maximum chip thickness. During tool entry, an impact load occurs on the rake face with high compressive stresses. The tool exit, on the other hand, is characterized by tensile stresses along the rake face resulting from chip-end. The loads on the cutting wedge are shown in Fig. 7.

To determine the stress during tool entry, the cutting and feed forces must be calculated according to the following equations (1) and (2).

$$F_{N,entry} = F_c \cdot \cos(\gamma) - F_f \cdot \sin(\gamma) \quad (1)$$

$$F_{T,entry} = F_c \cdot \sin(\gamma) + F_f \cdot \cos(\gamma) \quad (2)$$

At the time of entry, there is no relative movement between rake face and a chip and also no contact between cutting edge and workpiece surface. Therefore, the tangential forces approach zero and do not need to be considered further. There are only normal stresses present as triangular loads, with the maximum at the point of rake face contact furthest from the cutting edge. Accordingly, the maximum normal stress can be calculated by the equations (3) and (4).

$$\sigma_{N,entry} = 2 \cdot F_{N,on} / (Kl_{\gamma,entry} \cdot b) \quad (3)$$

with:

$$Kl_{\gamma,entry} = h / (\cos(\gamma)) \quad (4)$$

The stresses that occur during the continuous cut after the tool entry can be calculated according to Bergmann [4, 14]. The maximum calculated tangential stress at a cutting edge rounding of $\overline{S}$ = 30 µm is $\tau_{\varepsilon,max}$ = -1,250 MPa. For a rounding of $\overline{S}$ = 100 µm, the tangential stress is $\tau_{\varepsilon,max}$ = -380 MPa. As stated in [4] the maximum normal stresses are not critical in case of a continuous cut. The maximum normal stress at the tool entry increases from $\sigma_{N,exit}$ = 4,250 MPa ($\overline{S}$ = 30 µm) to $\sigma_{N,exit}$ = 4,320 MPa ($\overline{S}$ = 100 µm).

The tool exit must then be considered as a third stress case in addition to the tool entry and the continuous chip formation. Since in the case of the chip-end the chip no longer slides along the rake face, but the entire chip bends downwards, the acting tangential forces go to zero during the exit [13]. The load stress results from the normal force, which can be calculated according to (1) and must be related to the chip contact length during the tool exit $KL_{\gamma,exit}$. The resulting load stress can be assumed as a triangularly distributed surface pressure along the contact area as shown in Fig. 7 and can be calculated with the following equation (5) [13]. The normal stress at the tool exit increases from $\sigma_{N,exit}$ = 1,270 MPa ($\overline{S}$ = 30 µm) to $\sigma_{N,exit}$ = 1,350 MPa ($\overline{S}$ = 100 µm).

$$\sigma_{N,exit} = 2 \cdot F_{N,exit} / (Kl_{\gamma,exit} \cdot b) \quad (5)$$

In order to determine the cause of cutting edge failure and to prevent it during the process, the stresses inside the cutting tool need to be calculated and compared with the load limits of the cemented carbide. The temperatures and load stresses lead to the formation of compressive and tensile stresses in the cutting wedge, which exceed the strength of the cemented carbide and thus cause chipping on the cutting edge.

For the calculation of the cutting wedge stresses, a coupled simulation of a transient heat flux and a static stress simulation based on the finite element method is used. ANSYS Workbench 2019 R3 is used as the simulation environment. First, the temperature distribution in the cutting wedge is simulated in the transient heat flow simulation, based on the temperatures determined during machining. This heat distribution and the determined stresses along the cutting wedge are applied in the static stress simulation to consider the resulting mechanical and thermal stresses in the carbide. In the following, the most critical stress state of the cutting wedge was considered. The simulation model is shown in Fig. 8.

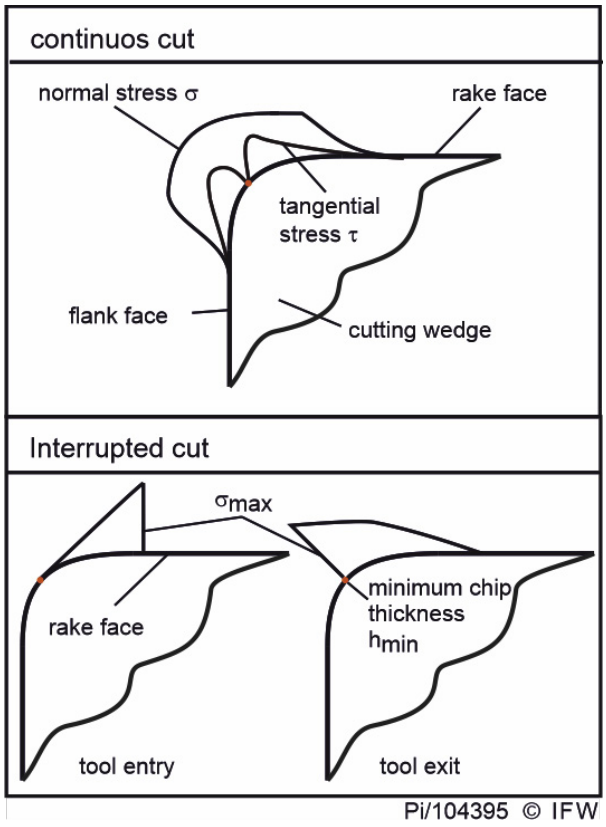

Fig. 7. Mechanical loads on the cutting wedge

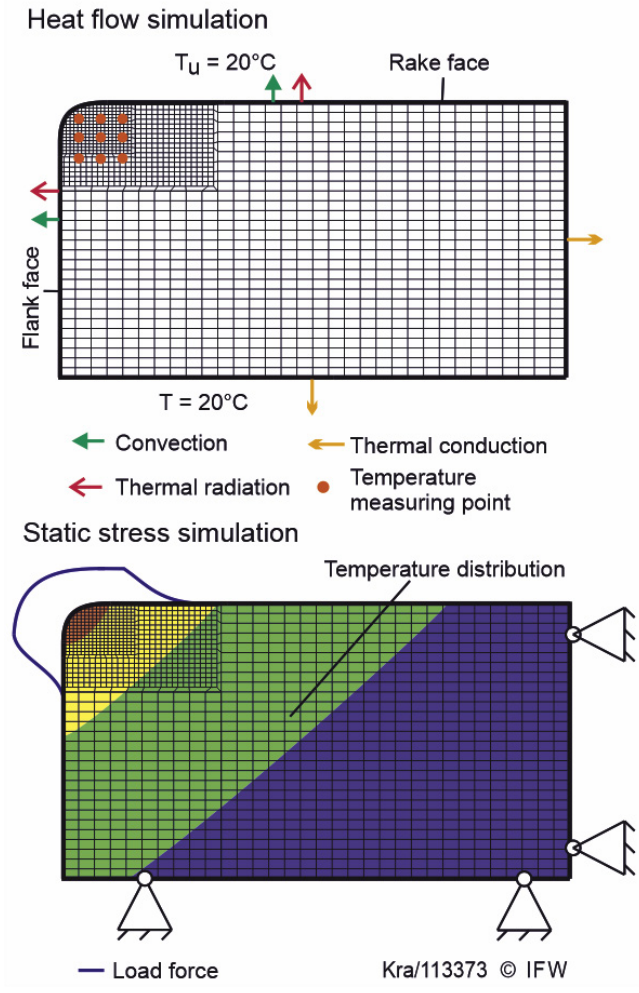

Fig. 8. Simulation of the mechanical and thermal stresses

Fig. 9 shows the simulated stresses in the cutting wedge for the tool entry and exit. The maximum compressive stress is 4,158 MPa at the tool entry. In this case this does not exceed the load limit of the cemented carbide at the corresponding temperature 4,242 MPa. For a cutting edge rounding of $S_\alpha = S_\gamma = 60$ µm, the stresses lie between the calculated values of the roundings $S_\alpha = S_\gamma = 30$ µm and $S_\alpha = S_\gamma = 100$ µm.

The simulation of the stresses on the cutting wedge shows that the breaking chip end and the normal stresses lead to tensile stresses in the area of the rake face. With a cutting edge rounding of $S_\alpha = S_\gamma = 30$ µm, the maximum tensile stress is 747 MPa during tool exit. For tensile stresses, the limits of cemented carbide are at 591 MPa. The tensile stress exceeds the load limit of the cemented carbide. The cutting edge cannot withstand the load, which leads to an initial cutting edge failure. The maximum tensile stress for a cutting edge rounding $S_\alpha = S_\gamma = 100$ µm is 380 MPa. This corresponds to a reduction of the load by almost 50%. The load is below the load limit of the cemented carbide. Consequently, no cutting edge failure occurs. The calculation results were validated in experimental investigations using tools with the corresponding cutting edge roundings.

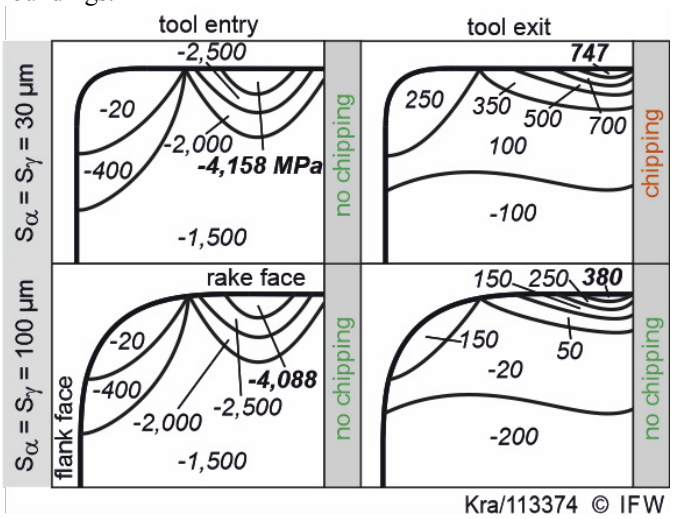

Fig. 9. Calculated stresses at the cutting wedge

5. Conclusions

On the basis of the investigations, it is now possible to calculate the stresses during tool entry and exit. These stresses can now be compared with the load limits of the cutting material. When the calculated stresses exceed the load limits, the cutting edge chipping occurs. Thus, it is possible to simulate the cutting edge chipping during interrupted cutting and therefore it is now possible to design the cutting edge microgeometry in a load-optimized way for processes with interrupted cuts. This knowledge enables the manufacture of more productive tools with longer tool life. The rounding $S_\alpha = S_\gamma = 100$ µm results in a stable cutting edge, while the cutting edge with a rounding of $S_\alpha = S_\gamma = 30$ µm failed during tool exit.

Based on the results, the following conclusions can be drawn:

- The process temperature increases with greater cutting edge roundings in processes with interrupted cutting
- Greater cutting edge roundings lead to reduced tensile stresses at the tool exit
- Cutting edge chipping occurs if the tensile stresses at the tool exit exceed the load limit of the cemented carbide

Acknowledgement

The authors would like to thank the Deutsche Forschungsgemeinschaft (DFG, German Research Foundation) for the funding of the projects 444577723 and 60442593.

References

[1] Denkena B., Biermann D.: Cutting edge geometries. CIRP annals - Manufacturing Technology, Vol 63, 2014, p. 631 - 653
[2] Denkena B., Reichstein M., Brodehl J., Leon-Garcia L.: Surface Preparation, Coating and Wear Performance of geometrically definded cutting edges. Proceedings of the 5th International Conference "The Coatings" in Manufacturing Engineering, 2005
[3] Bassett E.: Belastungsspezifische Auslegung und Herstellung von Schneidkanten für Drehwerkzeuge, Dr.–Ing. Dissertation, Leibniz Universität Hannover, 2014
[4] Bergmann B.: Grundlagen zur Auslegung von Schneidkantenverrundungen, Dr.–Ing. Dissertation, Leibniz Universität Hannover, 2017
[5] Biermann D., Aßmuth R., Hess S., Tiffe M.: Simulation base analysis and optimisation of the cutting edge micro shape for machining of nickel-base alloys. Procedia CIRP, Vol 67, 2018, p. 284-289
[6] Rehe M.: Herleitung prozessbezogener Kenngrößen der Schneidkantenverrundung im Fräsprozess. Dr.–Ing. Dissertation, Leibniz Universität Hannover, 2015
[7] Kato S., Yamaguchi K., Yamada M.: Stress Distribution at the Interface between tool and chip in machining, Journal of Engineering for Industry, 1972, p. 683 - 689
[8] Usui E., Kikuchi K., Hoshi K.: The theory of plasticity applied to machining with cut –away tools, 1964, p. 95 – 104
[9] Ulutan D., Özel T.: Determination of ttol friction in presence of flank wear and stress distribution based validation using finite element simulations in machining of titanium and nickel based alloys, 2013, p. 2217 – 2237
[10] Klocke F., König W.: Fertigungsverfahren 1: Drehen, Fräsen, Bohren. 8. Edition, Springer-Verlag, 2008
[11] Pekelharin: Cutting tool damage in interrupted cutting. Wear, Vol. 62, 1980, p. 37-48
[12] Pekelharin A.J.: The exit failure of cemented carbide face milling cutters Part I – Fundamentals and Phenomena. Annals of the CIRP, Vol. 33/1, 1984, p. 47-50
[13] Scherbath S.: Der Einfluss der Schneidkeilgeometrie auf das Zerspanverhalten beim Fräsen von Stahlwerkstoffen mit beschichtetem Hartmetall. Dr.–Ing. Dissertation, TUHH, 1998
[14] Bergmann B., Grove T.: Basic principles for the design of cutting edge roundings. CIRP Annals – Manufacturing Technology, Vol. 67, 2018, p. 73-78